JOURNAL OF COMPUTATIONAL PHYSICS 75, 283–299 (1988)

A Study of Nonlinear Radiation Damping by Matching Analytic and Numerical Solutions*

J. L. ANDERSON AND D. W. HOBILL

Department of Physics and Engineering Physics, Stevens Institute of Technology, Hoboken, New Jersey 07030

Received July 1, 1986; revised April 14, 1987

A linear oscillator coupled to a nonlinear field was studied using a mixed analytic-numerical matching scheme. An approximate causal solution was constructed in the radiation zone and matched to a numerical solution obtained using a finite differencing scheme in the inner zone. The requirement that the two solutions agree in the overlap region determined the arbitrary function in the retarded solution and at the same time allowed one to extend the numerical scheme arbitrarily into the future. The late time behavior of the system was investigated using a variety of initial conditions. In all the cases studied this behavior was found to be independent of which initial conditions were used. Also, it was shown that the linearized "monopole energy loss formula" breaks down in cases involving either fast motions or strong nonlinearities.

I. INTRODUCTION

Since they are nonlinear, the Einstein equations of general relativity are not easily integrated analytically. Only in very special cases can one actually find exact closed form solutions and it often turns out that such solutions defy any physical interpretation. In spite of this difficulty much information has been aquired through the use of approximate methods which formally expand the field equations in terms of some small expansion parameter. These approximation techniques then allow one to solve the equations iteratively taking the nonlinearities into account at progressively higher orders in the expansion parameter. This method has undergone considerable refinement in the past decades and has yielded such an exceptional agreement with the observed motions of the binary pulsar PSR 1913 + 16 that the system can be considered the first (indirect) observational evidence of the existence of gravitational radiation [1].

The important contribution that made this progress realizable was the recognition that the approximate analytic calculation could be simplified through the use of several expansion parameters. As a consequence one need not be restric-

* Work supported in part by NSF Grant PHY-8503879.

0021-9991/88 $3.00

581 75/2-3

ted to the construction of a single global solution dependent upon just one expansion parameter. Rather each of several expansion parameters defines an approximate solution that is valid in a limited region of the space-time. In addition the expansions that determine the solution in each limited region need not necessarily be the same. However, in the regions where two solutions overlap, one can identify certain arbitrary functions in one region with known functions in another, thereby matching the different solutions. With enough regions one can construct a solution that covers the entire space-time.

This procedure, known as the method of matched asymptotic expansions (MAE) [2], as powerful as it is, is limited by the requirement that the physical parameters of the system must be such that they yield small (compared to unity) dimensionless expansion parameters. In general relativity these expansion parameters may be a measure of the weakness of the gravitational field or the slowness with which source motions occur compared to the speed of light. Such methods unfortunately explore only a certain region of the parameter space available to more general solutions of the field equations.

Of course numerical methods can be used to avoid the restriction to small expansion parameters and this results in an exploration of a greater portion of the parameter space of solutions. At the present time, practical considerations require that numerical methods applied to the equations of general relativity be made as efficient as possible. In addition, once a numerical solution is generated it must in some way be subjected to stringent tests in order to determine whether or not it is physically reasonable. This is particularly crucial in cases where the numerical solutions depend upon certain physical parameters whose values may be presently beyond the values for which experimental verification can be made.

With these points in mind, we have begun a program that applies the philosophy of the method of matched asymptotic expansions to a technique that not only increases the efficiency of a numerical calculation but acts as a means of testing the consistency of the solution with reasonable physical assumptions. Simply stated, the procedure assumes that any relativistic system, consisting of a material source distribution confined for all time within a compact volume, and surrounded by empty space, can be described analytically in a region far from that source by a causal solution. By this we mean that if the source is stationary prior to some given time t_0, after which it becomes nonstationary and if, in addition, there exists in the exterior region a family of nonintersecting null cones labelled by the retarded coordinate u, then the field associated with the source is stationary for all retarded times prior to some retarded time u_0.

This notion of causality is of course required on physical grounds and leads to a unique form for the outer solution without the addition of such assumptions as the nonexistence of incoming radiation, or that the radiation must be everywhere outgoing. A purely outgoing condition will certainly not hold if there is backscatter of radiation due to background curvature and/or nonlinear interactions of the field. It has also been demonstrated that causal solutions do exist for simple systems that violate the requirement that there be no incoming radiation. In this paper we shall

be concerned with the evolution that follows from Cauchy data given on a $t = \text{const.}$ space-like hypersurface. We will not, however, raise the question of whether or not the initial data is consistent with the absence of incoming radiation at past null infinity.

The matching of a causal analytic solution to a numerical solution has been employed in problems that model the behavior of an isolated source emitting gravitational waves that eventually propagate out to null infinity. Such systems if left to themselves are subject to radiative damping. For the simple but well-known problem consisting of an oscillator coupled to a scalar field [3], it has been demonstrated that the numerical methods allow one to extend our knowledge of the behavior of the model beyond the limited parameter space for which one can obtain approximate analytic solutions. This was necessary in order to demonstrate that the "monopole energy loss formula" derived from a purely analytic application of the method of matched asymptotic expansions was only applicable for source motions that were slow compared to the velocity of light.

In a second application of the method it was shown that in the presence of background curvature, for which it could no longer be assumed that the radiation field was purely outgoing, one could derive an approximate analytic solution to the outer zone problem (in the region where the effects of the curvature become small). Furthermore, that solution could be effectively matched to a numerical solution obtained in the region immediately surrounding the source where the curvature was strong [4]. Not only did this method prove to be effective in increasing the efficiency of the numerical code by imposing a realistic boundary condition, but it also was useful in checking the accuracy of the numerical method within a large region where both the analytic and numerical solutions were valid. The fact that the analytic solution is connected directly to the boundary conditions at future null infinity helps solve the problem of how one characterizes the radiative part of the field in a local numerical calculation.

In this paper we shall continue to utilize the same method in a model problem that involves a nonlinear self interaction; namely a ϕ^4 theory. As in the curved space situation, the nonlinearity will not allow one to impose a purely outgoing radiation condition at finite distances from the source. Therefore an approximation procedure will be used to construct an analytic solution in a region far removed from the source. The validity of the approximate solution will extend from a finite radius out to future null infinity. A numerical solution can then be generated in the region containing the source and part of the empty space region surrounding it. In the region where the two solutions overlap the otherwise arbitrary functions appearing in the analytic solution can be matched to the numerical values they obtain in the region defined by the size of the finite differencing grid, thereby yielding a solution that covers the entire space-time.

In the next section we shall describe the analytic nature of the model problem and the method for determining the causal solution in the outer region. Section 3 will be devoted to the numerical methods used to calculate the behavior of the model in the source region where the nonlinearity is considered to be strong and

the motions rapid. In the final section we discuss the results of matching the numerical and analytic causal solutions and how one may use the latter to check the accuracy of the former over a rather large region of overlap.

II. The Model and Outer Zone Approximation

The model problem to be studied consists of a spherically symmetric scalar field $\psi(r, t)$ that is coupled to a nonrelativistic harmonic oscillator with an amplitude $Y(t)$. Since the Lagrangian of the system contains a term $(k/4)\psi^4$, representing the nonlinear self interaction of the field, the model is defined by the following system of equations.

$$(\partial_t^2 - \nabla^2)\psi + k\psi^3 = \lambda\rho(r)\, Y(t) \tag{2.1}$$

$$\partial_t^2\, Y + \omega^2 Y = \lambda \int_0^\infty 4\pi r^2 \rho\psi\, dr, \tag{2.2}$$

where ω is the uncoupled frequency of the oscillator, λ is the coupling constant, and k gives the strength of the nonlinearity. The source density is simply the Heaviside step function

$$\rho(r) = \Theta(1-r) \equiv \begin{cases} 1, & r \leqslant 1 \\ 0, & r > 1. \end{cases} \tag{2.3}$$

One now introduces the spherically symmetric function $\phi(r, t)$ defined by the relation

$$\psi(r, t) = \phi(r, t)/r. \tag{2.4}$$

It will be assumed that in some region outside of the compact volume surrounding the source there exists a family of nonintersecting null cones labelled by the retarded null coordinate $u = t - r$. One may now rewrite Eq. (2.1) in terms of ϕ and the variables r and u. In the vacuum region one has the homogeneous equation

$$(2\partial_u\, \partial_r - \partial_r^2)\, \phi + \frac{k\phi^3}{r^2} = 0. \tag{2.5}$$

An approximate solution to this equation can be constructed by expanding ϕ in successive powers of k,

$$\phi = \sum_{n=0} k^n \phi_n. \tag{2.6}$$

Therefore the first approximation to Eq. (2.5) is just the linear equation

$$(2\partial_u\, \partial_r - \partial_r^2)\, \phi_0 \tag{2.7}$$

which has as a solution

$$\phi_0 = \phi_0(u). \tag{2.8}$$

The second approximation to the wave equation is

$$(2\partial_u \partial_r - \partial_r^2)\,\phi_1 = \frac{-\phi_0^3}{r^2}. \tag{2.9}$$

Since ϕ_0 is independent of r this equation may be integrated once with respect to r to obtain

$$(2\partial_u - \partial_r)\,\phi_1 = \frac{\phi_0^3}{r} \tag{2.10}$$

and this equation has as a causal solution

$$\phi_1 = \int_{-\infty}^{u} \frac{\phi_0^3(u')\,du'}{(u-u'+2r)}. \tag{2.11}$$

Similar expressions may be obtained for the higher order approximations to the function ϕ. It can be seen that ϕ_0 is the generating function for all the other higher order terms in the expansion for ϕ. In this sense ϕ_0 may be considered equivalent to the "news function" [5] in a Bondi system of well-stacked null cones for general relativity. All information concerning the behavior of the system is contained in the function ϕ_0 and this uniquely determines the evolution of the system.

Since this simple problem is intended to model the behavior of the radiative part of the gravitational field, it must be emphasized that we are concerned here only with the purely radiative part of the scalar field as it propagates on a zero mean field background. The method of solution presented here of course is not applicable to the static nonlinear field. Just as the "news" in a general relativistic system vanishes for a stationary space-time, in the absence of a time dependent source term, $\phi_0 = 0$ here.

The dynamics of the system is known to be invariant to a rescaling of the field and the oscillator amplitude. If one defines the rescaled functions

$$\bar{\psi} = \psi/\alpha \qquad \text{and} \qquad \bar{Y} = Y/\alpha; \qquad \alpha = \text{const.}$$

then the nonlinear coupling constant $\bar{k}$ becomes $\bar{k} = k\alpha^2$ and the Eqs. (2.1) and (2.2) become

$$(\partial_t^2 - \nabla^2)\,\bar{\psi} + \bar{k}\bar{\psi}^3 = \lambda\rho\,\bar{Y} \tag{2.1'}$$

$$\partial_t^2\,\bar{Y} + \omega^2\,\bar{Y} = 4\pi\lambda \int_0^{\infty} r^2\rho\bar{\psi}\,dr \tag{2.2'}$$

while the parameters λ and ω remain unaffected. Unless otherwise specified, in the remaining sections it will be understood that we are dealing with the rescaled equations such that $\bar{k}$ is normalized to unity, and therefore the bars over the rescaled quantities will be dropped.

III. The Numerical Analysis of the Model

In this section we shall discuss the finite differencing scheme used to analyse the set of Eq. (2.1) and (2.2) in the region that contains the source and extends far enough into the vacuum region that it overlaps with a valid second-order approximation to the vacuum field equation. Given the initial values of the functions ϕ, $\partial_t \phi$, Y, and $\partial_t Y$ on a $t = \text{const.}$ space-like hypersurface, the field equation and the equation of motion for the oscillator amplitude uniquely determine the subsequent evolution of the model. At the present it will be assumed that the initial data is given as

$$\phi = \partial_t \phi = 0, \qquad Y = 0, \qquad \partial_t Y = \omega Y_0 \qquad \forall r \text{ at } t = 0. \tag{3.1}$$

Later, in order to determine the model's sensitivity to initial conditions, other sets of initial data will be employed. This test will be discussed in the next section.

The numerical solution to the system (2.1) is obtained using either of two different leapfrog finite differencing schemes. In both we introduce the function $f(r, t) = r\psi(r, t)$. Introducing the auxilliary function $g(r, t)$, the second-order wave equation may be written in the following as a system of equations where all derivatives (temporal and spatial) are of first order.

$$\partial_t f = \partial_r g - \frac{k}{r^2} \int_{\infty}^{t} f^3(t', r)\, dt' \tag{3.2a}$$

$$\partial_t g = \partial_r f + \lambda \int_0^r \rho(r')\, r' Y\, dr' = \partial_r f + \lambda Y \left(\frac{r^2}{2} - \frac{1}{2} \right) \Theta(1 - r). \tag{3.2b}$$

A simple grid on which the function $f(r, t)$ is evaluated at the integral space and time points and $g(r, t)$ is evaluated at the half-integral points can be set up. The numerical method of evaluating the time integral of the nonlinear term is, for the case of slowly varying fields, a simple trapezoidal scheme. For more rapidly varying systems, a higher order (e.g., Simpson's rule) integration scheme is employed in all calculations with $\omega \geqslant 1$. The finite differenced equations are then simply

$$f_J^{I+1} = f_J^I + \frac{\Delta t}{\Delta r} \left(g_{J+1/2}^{I+1/2} - g_{J-1/2}^{I+1/2} \right) - \frac{k}{2J^2} \left(\frac{\Delta t}{\Delta r} \right)^2 \sum_{m=0}^{I} \left[(f_J^m)^3 + (f_J^{m+1})^3 \right] \tag{3.3a}$$

$$g^{I+1/2}_{J+1/2} = g^{I-1/2}_{J+1/2} + \frac{\Delta t}{\Delta r}(f^I_{J+1} - f^I_J)$$

$$+ \frac{\lambda}{2}\Delta t[(J\,\Delta r)^2 - 1]\,\Theta(N-J)\,Y^I, \tag{3.3b}$$

where I and J label temporal and spatial grid points, respectively. The radial step size is chosen such that there is an integral number of steps, N, from $r=0$ to the boundary of the source.

A second, and more straightforward, method defines $h(r, t)$ as the time derivative of $f(r, t)$ and employs the second spatial derivative of $f(r, t)$. In this method both f and h are located at integral radial points. The leapfrogged evolution occurs with f evaluated on the integral time steps and h evaluated on the half integral time steps.

$$f^{I+1}_J = f^I_J + \Delta t\, h^{I+1/2}_J \tag{3.4a}$$

$$h^{I+1/2}_J = h^{I-1/2}_J + \frac{\Delta t}{(\Delta r)^2}[f^I_{J-1} - 2f^I_J + f^I_{J+1}]$$

$$- \frac{k\,\Delta t}{(J\,\Delta r)^2}(f^I_J)^3 + \lambda\,\Delta t\,\Delta r J\Theta(N-J)\,Y^I. \tag{3.4b}$$

The equation of motion (2.2) is also finite differenced using the leapfrog method (where Y and $\dot{Y}$ are evaluated on the integral and half-integral time steps respectively) and once again the integrals are evaluated either by the trapezoidal method or Simpson's rule depending upon the oscillator frequency.

The boundary conditions at $r=0$ are such that due to the spherically symmetric nature of the problem the function f and its time derivative must vanish for all time if it is to satisfy the initial conditions (3.1) at $r=0$. In the exterior region it will be required that the proper boundary conditions must accurately account for the true nonlinear propagation of the radiation occuring at a finite distance from the source.

The solution clearly must be outgoing at future null infinity and it is there that one has an unambiguous boundary condition. However, numerical schemes are limited to finite regions. While one could compactify the outer region such that "infinity is made finite" (a procedure that has been used in numerical studies of the characteristic initial value problem [6]) the value of numerical relativity lies in its ability to calculate the complicated dynamics in the source region.

In what follows we shall demonstrate that the second-order solution to the homogeneous equation derived in the previous section can provide an outer boundary condition at a finite distance from the source, thereby reducing both the amount of numerical and analytic work needed to obtain a global solution. This method increases the efficiency of the numerical code by limiting the number of grid points needed to carry out the computation and reduces the order of approximation needed in the analytic solution by performing the matching at an appropriate distance from the source. It will also be demonstrated that once the

boundary condition is set up, the matching of the analytic and numerical solutions can be used over a finite region to test the accuracy of both the numerical and analytic schemes.

Figure 1 represents the manner in which the retarded null cones are attached to the numerical grid at a radius r_m, called the matching radius. The numerical value of $f(r, t)$ is known at the intersection of r_m with the $t=\text{const}$ hypersurface. The arbitrary function of u appearing in the second-order approximate analytic solution for $\phi(u, r)$ is then determined by the same numerical value of f. Since Eqs. (2.8) and (2.11) express how the field propagates along the $u=\text{const.}$ null cones as a function of r, one can calculate analytically the value of the field at the point $(r_m+\Delta r_m, t+\Delta t)$ on the same null cone. This procedure of matching the arbitrary function in the analytic solution to the numerical solution for that same function determines a solution that is valid over the entire space-time.

Rewriting Eqs. (2.8) and (2.11) in their finite differenced form, the condition at the matching radius is

$$f(t, r_m)=\phi_0(u)+\frac{1}{2}k\,\Delta u\sum_{l=0}^{m-1}\frac{\phi_0^3(l\,\Delta u-1)}{(u+1-l\,\Delta u+2r_m)} \tag{3.5}$$

where the integer m is the number of null cone slices between the time that ϕ_0 first begins to change to the time at which the matching is performed.

Notice that the value g or h on the next half-time slice can be determined solely from the information on how the function f propagates along the null cone. This matching procedure therefore limits the types of finite differencing schemes that can be employed. Clearly (except in the case of linear propagation along flat null cones), it would be difficult to determine how the auxilliary functions g and h propagate along the null cones. Therefore finite differencing schemes that require a

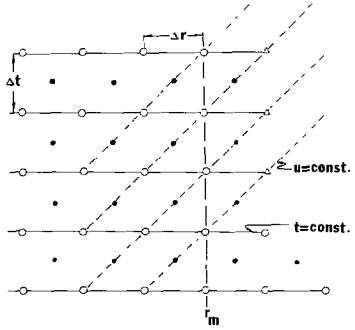

FIG. 1. The grid used for the leapfrog scheme, where the function f is calculated numerically at the positions represented by the open circles. The function g is calculated at the closed circle sites (or in the other scheme, h is evaluated on the $\frac{1}{2}$ time steps at the same spatial locations as f). When $\Delta t=\Delta r_m$ the null cones intersect the numerical grid at the integral time and space points. The matching procedure provides the boundary condition at the sites marked by the triangles.

knowledge of both f and g (or h) at the same space and time points must be excluded from the matching procedure. Examples of such methods are the first-order Lax scheme and the Lax–Wendroff scheme, both of which yield stable finite difference equations for wave equations.

While the present calculation uses $\Delta t = \Delta r$ throughout, Fig. 1 represents a grid for a more general situation where $\Delta t \neq \Delta r$ at r_m. Depending upon the null cone structure (i.e., in situations where the null coordinate $u \neq t - r$) and/or the stability requirements (e.g., Courant conditions) of the differencing scheme, the ratio $\Delta t/\Delta r_m$ need not be unity or even constant at each time slice. All that is required is that the values of $f(r_m, t)$ and $f(r_m + \Delta r_m, t + \Delta t)$ be such that they lie along a $u = \text{const.}$ nonintersecting null cone and on two successive time slices. The values of Δr_m and Δt can always be adjusted to meet that requirement. A discussion of the interpolation methods used to accomodate varying grid spacings can be found in Ref. [4], where matching conditions in curved space-times are considered.

For a problem such as the one considered here, there is a price to pay. The analytic solution is given in terms of an integral over the entire time that ϕ undergoes its evolution. While the causal solution is therefore nonlocal in that it depends upon its entire past history, its ability to "remember" that past fades over time. From a practical point of view one can truncate the summation process in the evaluation of the integrals over the previous history since the major contribution to the sum in Eq. (3.4) comes from values not far removed from the retarded time at which the matching is performed. Clearly the expression in the denominator grows as $u - u'$. Therefore only a finite number of elements need to be included in the integral expression for the second-order solution.

In addition to providing a realistic boundary condition, the procedure outlined above can be considered to be a true matching of the numerical and analytic solutions in the finite region where the validity of the two solutions overlap. Thus

mine the solution at grid points located inside the matching radius. Knowing the value of the solution at r_m, one can follow the family of null cones farther in toward the source (provided that the corrections of order $1/r$ are small compared to the accuracy of the numerical solution) and check the consistency of the numerical values of the function $f(r, t)$ at the points at which the null cones intersect the $t = \text{const.}$ time slices.

This method of checking the accuracy of both the numerical and analytic solutions has a further advantage in that it is not just a check of the numerical solution but also allows one to determine the region over which the analytic solution is valid. Once the numerical and analytic solutions are shown to agree over a finite range of values of r, then the value of the matching radius can be chosen as the minimum value for which agreement can be found. This further increases the efficiency of the matching method for a numerical calculation by decreasing the number of necessary grid points.

IV. Numerical Results and Discussion

The system examined here, like the linear models studied in Refs. [3, 4] undergoes damping due to the emission of radiation as long as the coupling between the source and the field is not too large. For large values of λ, the energy of the system will not be positive definite and an instability results. This peculiarity exists in all models where the field and the source are coupled in the manner prescribed by Eq. (2.2) and has been discussed in previous work [3]. For the remainder of this paper it will be assumed that λ is small enough to ensure that the oscillator is always damped. For such problems there exist two quantities of physical interest: the damping "constant" β and the oscillator frequency, $\bar{\omega}$. The values of these two quantities can be found directly by fitting the numerical solution for the oscillator amplitude to a solution of the form

$$Y = Y_0 e^{-\beta t} \sin \bar{\omega} t. \tag{4.1}$$

In general both β, the damping term, and $\bar{\omega}$ are time dependent functions, but, for late times or sufficiently small values of λ they approach constant values. It is these values that we wish to determine.

Testing the Matching Methods.

As a preliminary test of the accuracy of the matching technique and a demonstration of the scale invariance, the behavior of the solution under rescaling was examined. As was expected the values of β and $\bar{\omega}$ were independent of scaling and depended only on the parameters λ and ω. The effect of scaling can be seen in Fig. 2, where the oscillator amplitude is plotted as a function of time. The damping term and the frequency of the oscillator determined from Eq. (4.1) are equal to within 0.05% for both runs: one where $\bar{k} = 4$, $\bar{Y}_0 = 0.5$ and the other where $k = 1$, $Y_0 = 1$. In both cases the values of λ and ω are the same. As expected, the field ϕ exhibits the same scaling relation as the amplitude. This scaling behavior was obeyed by both of the finite differencing schemes presented in the previous section.

A comparison of the differences in the values of β and $\bar{\omega}$ that resulted from using the two numerical schemes was made and it was found that the direct method

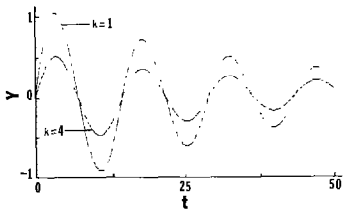

FIG. 2. An example of the scale invariance of the nonlinear oscillator equations under the transformation $k = \bar{k}/\alpha^2$, $Y = \bar{Y}\alpha$, and $\phi = \bar{\phi}\alpha$ for $\alpha = 2$. The step sizes are $\Delta t = \Delta r = \frac{1}{10}$ with $Y_0 = 1.0$, $\omega = 0.5$, $\lambda = 0.2$, and $r_m = 20$. The values of β and $\bar{\omega}$ agree to within 0.05%.

which utilized the second radial derivative was subject to a greater damping and dispersion than was the method that used the first derivatives with respect to the radial distance. The results of the second derivative scheme were also affected more by changes in step size. While a decrease in the step sizes (from 1/10 to 1/80) did not significantly change the behavior of the oscillator as calculated by the method using the function g, the evolution calculated with h approached that determined by the former with decreasing step size. Nontheless, even at the crudest spacing ($\Delta r = \Delta t = 1/10$) the differences in β were always less than 5% while the differences in $\bar{\omega}$ never exceeded 1%. Figure 3 shows an example of the differences that resulted from a calculation of the oscillator amplitude using the two methods. Since the two numerical methods behaved similarly to the tests that compared effects of matching to the first- and second-order approximate analytic solutions, we shall not give the results of both methods in order to avoid redundancy. The sample calculations that are presented in this work will be taken from the first-order spatial derivative method.

One of the first tests to be performed on the model was a comparison of the differences in the oscillator behavior resulting from matching the numerical solution to both the first- and second-order approximate analytic solutions at different radii. The calculations were carried out with fixed values of λ and ω. The matching radius was allowed to vary in the range $5 < r_m < 40$ for both the first- and second-order approximations and the evolution was allowed to proceed to $t = 500$ at which time the variation in the parameters of interest was less than a few parts in 10^5 between each oscillation.

The results from calculations performed on a DEC system 1090 (using a Fortran-77 compiler with a 32-bit single precision default) are shown in Table I. Included in the table are the CPU times needed to carry out the calculations. To increase the efficiency the sum appearing in Eq. (3.5) was truncated to include only those field values that preceeded the matching time by $50/\Delta u$ time steps. For comparison, a single calculation was performed where the integral in the second-order solution was evaluated over the entire dynamical history of the model and the information associated with that calculation is included.

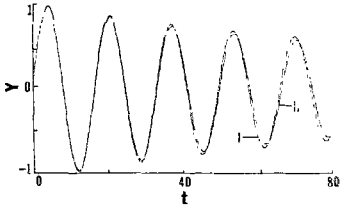

FIG. 3. A comparison of the two differencing schemes presented in Section III for an oscillator with $\omega = 0.4$, $\lambda = 0.1$, $Y_0 = 1.0$, with $r_m = 20$. The step sizes for the calculation are $\Delta t = \Delta r = \frac{1}{10}$. The curves labelled I and II plot, respectively, the schemes that use the first-order and second-order spatial derivatives. The differences between the values of β and $\bar{\omega}$ calculated using the two methods scales directly with the scaling in the step size.

At first sight it would appear that the corrections due to the nonlinear interaction are negligible, particularly at large matching radii. However, it is at intermediate times that the differences in the evolution resulting from different matching conditions become evident. For this reason the values of β and $\bar{\omega}$ at $t=100$ also included in Table I. The fact that the matching procedure significantly affects the intermediate time behavior of the oscillator is due to the following: At early times both the first- and secon-order approximations agree to within 0.01% simply because the second-order integral does not make an appreciable contribution to the solution until enough time has passed to record the nonvanishing history of the field evolution. The differences between the first- and second-order approximations are therefore the greatest when the field obtains its largest amplitude. At much later times the field has been damped to such a small value (less than unity) that the cubic nonlinearities make the contributions (to the second-order integral) from the immediate past very small. In addition, the contributions coming from the larger field values are diluted by the fact that they had occurred far enough in the past that the term $u-u'$ appearing in the denominator is large.

The integral appearing in the second-order approximation takes into account the backscatter due to nonlinear effects and a similar situation exists in a model described by a linear wave equation embedded in a fixed curved background spacetime [4]. In that case, however, the effects of backscatter are more pronounced since the nonzero curvature introduces a linear, rather than cubic, dependence on ϕ

TABLE I

Results of Different Matching Conditions

	$\omega=0.4$		$\lambda=0.2$		$Y_0=15.0$
r_m	$\bar{\omega}$ $t=500$	β $t=500$	$\bar{\omega}$ $t=100$	β $t=100$	Time(CPU)
a. *First approximation*					
5.	0.30784	0.022342	0.31401	0.020021	0:30.19
10.	0.30784	0.022609	0.31342	0.020007	0:50.99
20.	0.30783	0.022987	0.31352	0.019916	1:32.15
40.	0.30783	0.023088	0.31355	0.019938	2:58.93
b. *Second approximation*					
5.	0.30784	0.023608	0.31389	0.019244	0:53.85
10.	0.30784	0.022672	0.31357	0.019749	1:14.67
20.	0.30783	0.023132	0.31372	0.019740	2:03.07
40.	0.30783	0.023209	0.31370	0.019700	3:25.74
c. *Second approximation (over entire dynamical history)*					
20.	0.30783	0.023206			14:06.72

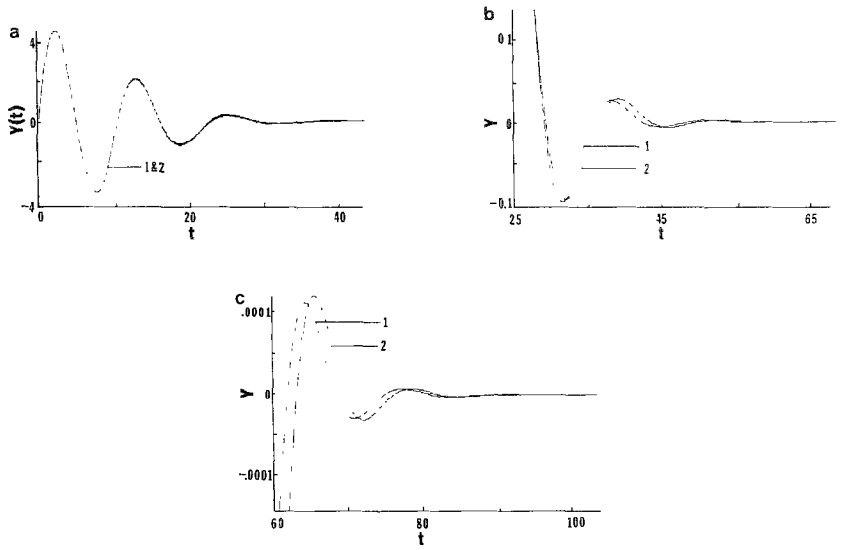

FIG. 4. The effects of matching to the first- and second-order approximate solutions (curves labelled "1" and "2", respectively) at $r_m = 40$. Here $Y_0 = 4.0$, $\omega = 0.8$, and $\lambda = 0.6$. Initially (a) the two methods are in agreement until (b) the second-order integral is large enough to make its contribution felt. After the field has damped to such an extent (c) that the nonlinerity becomes unimportant, the late time dynamics differ only by a constant phase ($\Delta t = \Delta r = \frac{1}{20}$).

in the integral and the background, being fixed, does not decay in time. Figure 4 shows what happens to the oscillator behavior when the second-order integral is ignored compared to matching the numerical solution to the complete second-order solution. In agreement with Table I it can be seen that at intermediate times the

At very late times, the perturbations due to the differences in the approximations are damped out enough that the asymptotic values of β and $\bar{\omega}$ are equal to within 0.01%. However, the phase difference that develops as a result of the different matching procedures remains fixed at a constant value during the late time evolution.

A demonstration of the consistency of the matching method is given in Table II. Since the analytic solution is known as a function of r and t, one may determine the solution at other points on the numerical grid. The easiest points to determine are those that lie along the characteristic surfaces. Therefore the location of the field points given in Table II are located on the null cones.

The differences between the second- and first-order approximations are of the order of ϕ_0^3/r and for late times these differences are small if the damping of the oscillator is significant. The results shown in Table II are chosen to coincide with the early and intermediate time scales where the differences are most noticable. The (single precision) numerical values of the function $f(r, t)$ are given together with the values of the second-order integral along chosen null cones at various fixed values

TABLE II

Matching the Numerical and Analytic Solutions along the Null Cones

u	t_1	$f\times 10^{-2}$ $\phi_1\times 10^{-2}$ $(r=10)$	t_2	$f\times 10^{-2}$ $\phi_1\times 10^{-2}$ $(r=20)$	t_3	$f\times 10^{-2}$ $\phi_1\times 10^{-2}$ $(r=30)$	t_4	$f\times 10^{-2}$ $\phi_1\times 10^{-2}$ $(r=40)$
0	10,	3.955130 0.000000	20,	3.955130 0.000000	30,	3.955130 0.000000	40,	3.955130 0.000000
10	20,	−3.110119 0.000039	30,	−3.110136 0.000023	40,	−3.110144 0.000016	50,	−3.110148 0.000012
40	50,	1.420980 −0.000007	60,	1.421011 0.000005	50,	1.421011 0.000004	60,	1.421011 0.000004
80	90,	1.773833 0.000012	100,	1.773832 0.000011	110,	1.773832 0.000008	120,	1.773830 0.000006
120	130,	1.501759 0.000006	140,	1.501756 0.000005	150,	1.501754 0.000004	160,	1.501752 0.000003

of r. At early times the solution is purely outgoing and at later times when the $u-u'$ term appearing in the second-order integral is small the corrections are approximately described by $F(u)/r$, where $F(u)=\frac{1}{2}k\int_0^u \phi_0^3\,du'$. At later times the second-order correction becomes a more complicated function of u and r but eventually damps out to a constant value. The fact that the numerical values of the field are not constant along a chosen null cone demonstrates the necessity of including the corrections to the purely outgoing vacuum solution if the matching is to be performed near the source.

The importance of matching to the correct analytic solution can clearly be seen for a linear field, where the general solution to the homogeneous equation is $\psi=\phi_{\text{ret}}(u)/r+\phi_{\text{adv}}(v)/r$. Here v is the ingoing null coordinate. One could very well have chosen a differencing scheme that used the advanced solution as a boundary condition. However, it would then be found that the numerical solution would not be constant along a chosen incoming null cone. If the problem is such that it evolves into the future from given initial data that is nonzero only in the finite region bounded by the numerical grid, then one is forced to accept the retarded solution as giving not only the outer boundary condition but the proper matching as well.

Dependence on Initial Data

As mentioned previously, a characteristic of all models employing a coupling of the kind given in Eq. (2.2) is that they undergo damping for small amplitude oscillations and small coupling constants. That they are also insensitive to changes in the initial conditions can be easily demonstrated experimentally by imposing different Cauchy data. The one requirement is that the initial total energy given by

$$E_{\text{total}}=\int d^3\times\left\{\frac{1}{2}(\partial_t\psi)^2+\frac{1}{2}(\nabla\psi)^2-\lambda Y\rho\psi+\frac{k}{4}\psi^4\right\}+\frac{1}{2}\left[(\partial_t Y)^2+\omega^2Y^2\right] \quad (4.2)$$

must be finite. Therefore, nonzero field values in a finite spatial region were introduced into the initial data (e.g., $\phi = \phi_0 \theta(r - r_0)$) as were nonzero values of its derivative. The changes in the values of β and $\bar{\omega}$ were only noticable on a time scale of the order of the light crossing time across the distance over which the field or its derivative were nonzero. As long as the initial conditions for ψ and $\partial_t \psi$ vanish outside of some region bounded by $r_0 \leqslant r_m$ the system always damped to the same values of β and $\bar{\omega}$ for given values of λ and ω.

The significance of the above is important. If our model reflects many of the properties of a system such as the binary pulsar then our lack of knowledge concerning the initial conditions of radiatively damped systems need not be of too great a concern as long as those initial conditions are physically reasonable and consistent with isolation of the system. Since generic initial conditions such as those given by Eq. (3.1) must include some "incoming radiation," the characterization of a non-incoming radiation initial condition is not important to the late time evolution of the system. This behavior is consistent with the conjecture by Schutz [8] that isolated radiating systems will undergo damping (after the time needed for light to traverse the compact source) for all but a very special class of initial conditions.

Related to this point is the fact that small perturbations occurring during the evolution of the system (in the case at hand these come from imprecise matching conditions) eventually damp out and these too are relatively unimportant to the late time behavior of the model. Therefore it would seem that in most long-lived astrophysical systems, dominated by the gravitational interaction, the presently observed evolution could have evolved from any number of initial conditions or even from any number of different evolutionary scenarios. The "fading memory" aspect of the causal solutions, however, leads to asymptotically similar solutions.

Linear vs *Nonlinear Effects*

Finally the effects of the nonlinear self-interacting field were compared to the linear model previously studied in Ref. [3]. Figure 5 shows that the damping of the oscillator is more pronounced for the nonlinear case than it is for its linear counterpart when the value of the coupling λ is large enough to be close to the value for

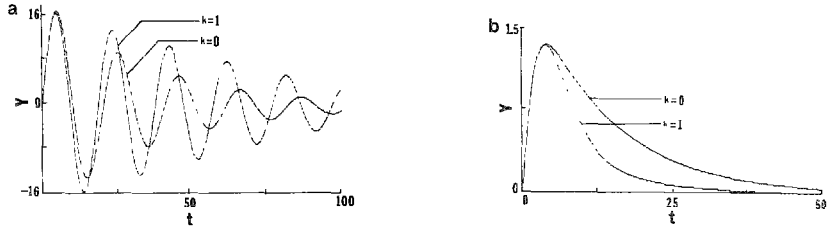

FIG. 5. The difference in behavior between the linear and nonlinear oscillator for (a) the underdamped case where $\omega = 0.4$, $\lambda = 0.2$, and $Y_0 = 16.0$ and for the (b) the critically damped linear oscillator where $\omega = 0.8$, $\lambda = 0.6$, and $Y_0 = 1$. At the value of λ for which the linear model becomes unstable ($\lambda \sim 0.625$), the nonlinear oscillator remains overdamped and only becomes unstable at $\lambda \sim 0.647$. In both cases $r_m = 20$ and $\Delta t = \Delta r = \frac{1}{10}$.

critical damping. This also means that the nonlinear oscillator is also more stable. That this is the case can be seen also by noting that at the critical value of the coupling for which the linear oscillator becomes unstable and blows up exponentially, the nonlinear oscillator continued to be damped. This is due to the addition of the positive definite energy density contribution coming from the quartic nonlinearity in the hamiltonian. Since similar (though quadratic) nonlinearities appear in general relativity it would seem that the gravitational radiation damping of a system could render marginally stable Newtonian systems stable.

As in the case of the linear model, the problem described here can also be studied for rapidly oscillating sources (even in the relativistic limit). Such situations cannot be analyzed by purely analytic approximation techniques alone. Only a numerical solution in the source region is capable of handling the complications associated with such motions. The analytic solution, on the other hand, makes the necessary connection of the numerical solution to regions far removed from source. In Ref. [3] it was demonstrated that the "slow motion monopole energy loss formula" derived from an energy balance equation that related the energy loss in the source region to the energy flux measured far from the source broke down for rapidly oscillating sources. This formula is similar to the linearized quadrupole energy loss formula derived for isolated slow-motion general relativistic sources. In addition to being invalid for fast motions, the linearized energy loss formula breaks down when the nonlinearities become important. This behavior is shown in Fig. 6.

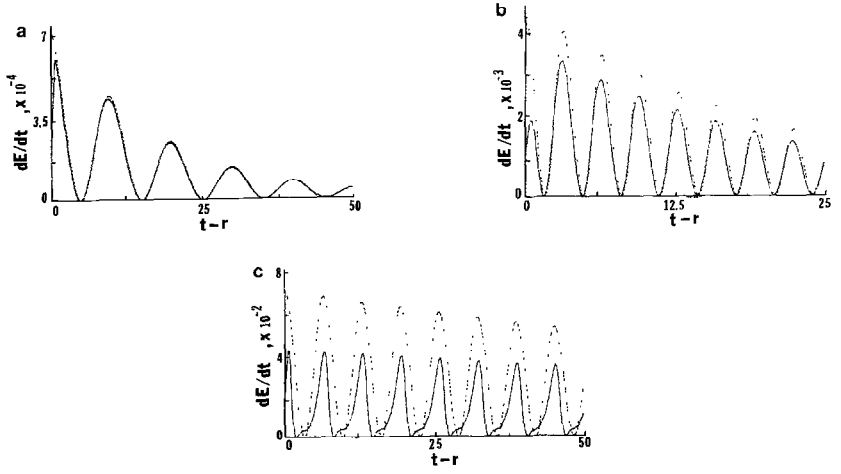

FIG. 6. The energy loss rate calculated from the change in the oscillator amplitude, Y (dotted lines) and compared to the rate determined from the far field at $r_m = 20$ (solid lines). The energy balance equation is derived from an analytic application of the MAE technique and is restricted to slow source motions and weak nonlinearities. Therefore it is valid for in the case (a), where $\omega = 0.4$, $\lambda = 0.2$, $Y_0 = 1.0$, and $k = 1.0$. For fast motions (b) with $\omega = 1.0$, $\lambda = 0.2$, $Y_0 = 1.0$, and $k = 1.0$, the energy balance formula breaks down as it does for the strongly nonlinear case (c) given by the parameters $\omega = 0.5$, $\lambda = 0.1$, $Y_0 = 16.0$, and $k = 4.0$.

The energy balance equation derived from the method of matched asymptotic expansions [7] can be written in the form

$$\frac{\lambda^2}{q}\left(\frac{\partial Y}{\partial t}\right)^2 = \left(\frac{\partial \phi_0}{\partial u}\right)^2, \tag{4.3}$$

where the left-hand side of the equation represents the energy loss resulting from the change in the oscillator amplitude and the right-hand side represents the energy loss determined from the flux of radiation through the spherical surface surrounding the source with a radius large compared to the source radius. Figure 6a shows a comparison of the two methods of calculating the energy loss for a slow motion weakly nonlinear system. Initially the two calculations do not agree but within one light crossing time it can be seen that Eq. (4.3) is valid to a high degree of accuracy. Figures 6b and c demonstrate the energy loss calculations for a fast motion source and a strongly nonlinear system, respectively. In both cases the source energy loss exceeds the energy loss calculated from the far field flux.

In conclusion it has been demonstrated that the method of matching a numerical solution to a known general approximate or exact analytic solution for a certain problem in a region where the two solutions overlap is advantageous to both methods. The numerical solution allows one to explore regions of the parameter space inaccessable to analytic techniques alone. In addition the form of the analytic solution is specified by the criterion that the two solutions must match over a finite region of space-time. The analytic solution (if it does not restrict the numerical methods employed) can be very effective in improving the efficiency of the numerical calculation as well as characterizing the physically significant quantities that eventually will be measured by experimental means.

REFERENCES

1. J. H. TAYLOR AND J. M. WEISBURG, *Phys. Rev. Lett.* **52**, 1384 (1984).
2. W. L. BURKE. *J. Math. Phys.* **12**, 254 (1971).
3. J. L. ANDERSON AND D. W. HOBILL, *Gen. Relativ. Gravitation* **19**, 563 (1987).
4. J. L. ANDERSON AND D. W. HOBILL, in *Dynamical Spacetimes and Numerical Relativity*, edited by J. Centrella (Cambridge U. Press, Cambridge, 1986).
5. H. BONDI, M. G. J. VAN DER BURG, AND A. W. K. METZNER, *Proc. R. Soc London A* **269**, 21 (1962).
6. R. ISAACSON, J. WELLING, AND J. WINICOUR, *J. Math. Phys.* **24**, 1824 (1983).
7. J. L. ANDERSON, *Gen. Relativ. Gravitation Proc. Int. Conf.* **15**, 595 (1983).
8. B. F. SCHUTZ, *Phys. Rev. D* **22**, 249 (1980).